IEEE Access
Multidisciplinary | Rapid Review | Open Access Journal

Received November 25, 2019, accepted December 5, 2019, date of publication December 10, 2019,
date of current version December 23, 2019.

Digital Object Identifier 10.1109/ACCESS.2019.2958604

A Contact-Based Data Communication Technique Using Capacitive Touch Screen Panel and Support Vector Machine Classifier

KI-HYUK SEOL, SEUNGJUN PARK, AND HYOUNGSIK NAM, (Member, IEEE)
Department of Information Display, Kyung Hee University, Seoul 02447, South Korea

Corresponding author: Hyoungsik Nam (hyoungsiknam@khu.ac.kr)

This work was supported in part by the IDEC (EDA Tool), and in part by the National Research Foundation of Korea (NRF) funded by the Ministry of Science, ICT, and Future Planning, under Grant NRF-2016R1A2B4009787.

ABSTRACT This paper demonstrates a data communication technology based on the capacitive touch screen scheme that can discriminate stylus and finger using a support vector machine (SVM) classifier. The transmitter in a stylus sends the binary data with no-touch and stylus-touch and the receiver in a touch screen panel (TSP) recovers the received data contents. In addition, the proposed transmission protocol implements an artificial finger-touch on the stylus side for initial and terminal codes. Furthermore, to compensate for common-mode drifts caused by HUM noises, upward and downward drift compensation circuits are proposed for the Tx pulse sensing circuit of the transmitter. The proposed method is evaluated by means of 8-inch capacitive TSP, programmable system-on-chip board, and host processor board. It is verified that the proposed method can support the high data rate of 100 bit per second (bps) or more with less bit error rate than 10^{-7}, compared to several bps of previous touch-based communication techniques.

INDEX TERMS Contact-based communication, SVM classifier, drift compensation, capacitive TSP.

I. INTRODUCTION

The mutual capacitive touchscreen technology has been adopted for most mobile devices due to its convenience and intuitiveness. As a result, it has become common that users deal with devices by touching a screen with their fingers these days. A conventional mutual capacitive touchscreen panel (TSP) is implemented as the array of mutual electrostatic capacitors formed at the intersection regions of transmitting (Tx) electrodes and receiving (Rx) electrodes [1], [2]. In general, Tx drivers sequentially send pulses to Tx lines and charge amplifiers receive those pulses on Rx lines through mutual capacitors. Because finger touches cause the changes of mutual capacitances, the output voltages of charge amplifiers become different from the voltage levels of the case that nothing is touched on the screen. This difference allows the touch to be discriminated. The output voltages are transformed into digital values by an analog to digital converter (ADC), and the touch position is computed on the host processor. To improve the signal-to-noise ratio (SNR) for the higher detection accuracy, multiple Tx pulses are sent over one touch point and the voltage difference between adjacent Rx lines are utilized [3]–[7].

In addition to finger touch sensing, various types of other input tools for touchscreens have been studied and developed to support more elaborate works such as writing texts and drawing pictures [8]–[13]. At present, a representative technology is a stylus that has been widely used in laptops, tablet PCs, and smartphones. The simplest method is a passive stylus based on conductor fibers to mimic fingers [8], therefore, it is difficult to distinguish a stylus from a finger. Active stylus technologies, on the other hand, are able to facilitate more sophisticated works by sending pulses to the TSP at the same timing as Tx pulses, transmitting different frequency pulses, and using the electromagnetic resonance technology [9]–[13]. Although these methods allow the TSP to distinguish the stylus from the finger and to fulfill sophisticated works, they cannot avoid increasing power consumption, operation complexity, hardware complexity, and cost. As another active stylus approach, a support vector machine (SVM) based scheme has been proposed to enable finger and stylus discrimination for sophisticated works

The associate editor coordinating the review of this manuscript and approving it for publication was Ting Wang.

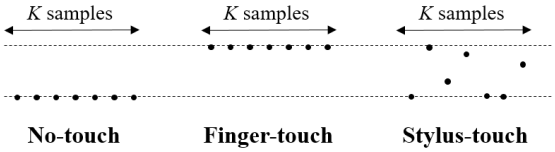

FIGURE 1. ADC sampling operations for three touch cases. Dots represent samples by an ADC.

without adding layers, increasing operation modes, and hardware complexity [14]. Finger and stylus are detected simultaneously and discriminated on one platform of a SVM classifier. This finger and stylus discrimination capability is required for the palm-rejection.

On top of the stylus and finger discrimination, there have been researches that try to transmit the data through the TSP for user identification and authentication [15], [16]. However, the previous asynchronous data transmission scheme applies lower frequency signals than Tx pulses of the TSP to generate artificial touch events. Furthermore, several touch events should be detected in the TSP processor for one-bit data determination, leading to very low data transmission rate of several bit per second (bps). Because the artificial touch generated by the transmitter is equal to the finger-touch in the receiver side, the transmitted data cannot be discriminated from finger-touches. Therefore, when fingers are placed on the TSP at the same time, the transmitted data cannot be properly decoded.

Meanwhile, this paper proposes a highly efficient contact-based data transmission technique that can achieve the higher data rate than previous methods by a factor of 10 and more and fulfill the data transmission even when fingers are touched on the screen simultaneously by means of the SVM-based stylus touch scheme. By sensing Tx pulses of the TSP, the proposed data transmission is synchronized to the reporting rate that is a maximum possible data rate at one contact point. Additionally, its data protocol allows the TSP to differentiate the transmitted data from the stylus-touch. Lastly, prototype systems and possible applications are introduced.

II. PROPOSED CONTACT-BASED DATA COMMUNICATION

In the SVM-based capacitive TSP [14], because a stylus transmits higher frequency pulses than Tx pulses, three different sequences of K samples such as no-touch, finger-touch, and stylus-touch are generated by the ADC of a Rx side as shown in Fig. 1. Then, these three sequences are discriminated through a SVM classifier that is a very efficient classifier especially in non-linear problem by comparing the distance with support vectors [17]. Consequently, even when both stylus and finger are placed on the screen, they are recognized separately.

The Rx circuit model of the SVM-based capacitive TSP can be described with a mutual capacitor (C_M), a stylus capacitor (C_{ST}), charge amplifier, ADC, and SVM classifier as presented in Fig. 2. A finger-touch reduces C_M, while C_{ST} is added only by a stylus-touch. The output voltages of the

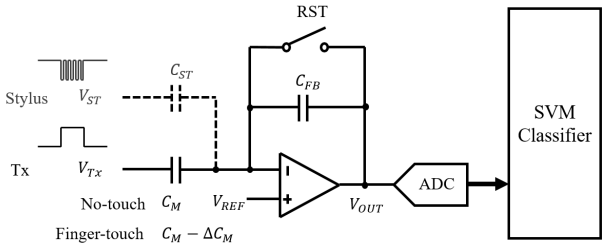

FIGURE 2. Rx circuit structure for a SVM-based capacitive TSP.

charge amplifier for no-touch and finger-touch (V_{OUT-NT}, V_{OUT-FT}) are presented in Fig. 3(a), where the C_M reduced by the finger-touch is represented as a smaller voltage swing than the no-touch case. Red dots are sampling points of the ADC. The output voltage for the SVM stylus-touch (V_{OUT-ST}) is illustrated in Fig. 3(b), where V_{ST} are the pulses generated by the stylus and various levels of voltages between V_{OUT-FT} and V_{OUT-NT} are sampled for Tx pulses leading to three classes of sequences for the SVM classifier. In addition, an artificial finger-touch can be also made up by an active stylus as shown in Fig. 3(c) [9], [10]. By applying the opposite polarity pulses to Tx pulses, the output voltage (V_{OUT-AF}) equivalent to V_{OUT-FT} is realized, therefore, this artificial finger-touch cannot be differentiated from the finger-touch. To cope with the different output voltage swing of the artificial finger-touch from that of the finger-touch, the sample data are saturated at the finger-touch value for enough large voltage swings of the stylus. This guarantees that artificial finger-touches are considered as finger-touches. As a result, the stylus can give rise to three cases of no-touch, stylus-touch, and artificial finger-touch that are utilized in the proposed data communication.

In the proposed SVM-based touch data communication system, the transmitter of a stylus sends the binary data stream with two levels of no-touch and stylus-touch at an on-off keying (OOK) modulation [15]. These transmitted data should be distinguished from stylus-touches and the multi-bit words should be correctly obtained from the bit stream. Therefore, the initial and terminal codes are added to the beginning and end of the data contents including the artificial finger-touch as shown in Fig. 4. Because data contents are binary signals of no-touches and stylus-touches, initial and terminal codes are perfectly identified. 0, 1, and 2 are linked to no-touch, stylus-touch, and artificial finger-touch, respectively. Since only two levels of no-touches and artificial finger-touches are available for all transmitted signals in the previous approach, long initial and terminal codes are required to be differentiated from data contents as presented in Fig. 5 [16]. Whereas, because the proposed scheme can utilize a ternary stylus signal of three values such as 0, 1, and 2, only short initial and terminal codes are sufficient with each length of 2 trits such as 12 and 02, respectively, where a trit is a ternary signal digit. Consequently, the proposed protocol is much more efficient than the previous capacitive touch data protocol.

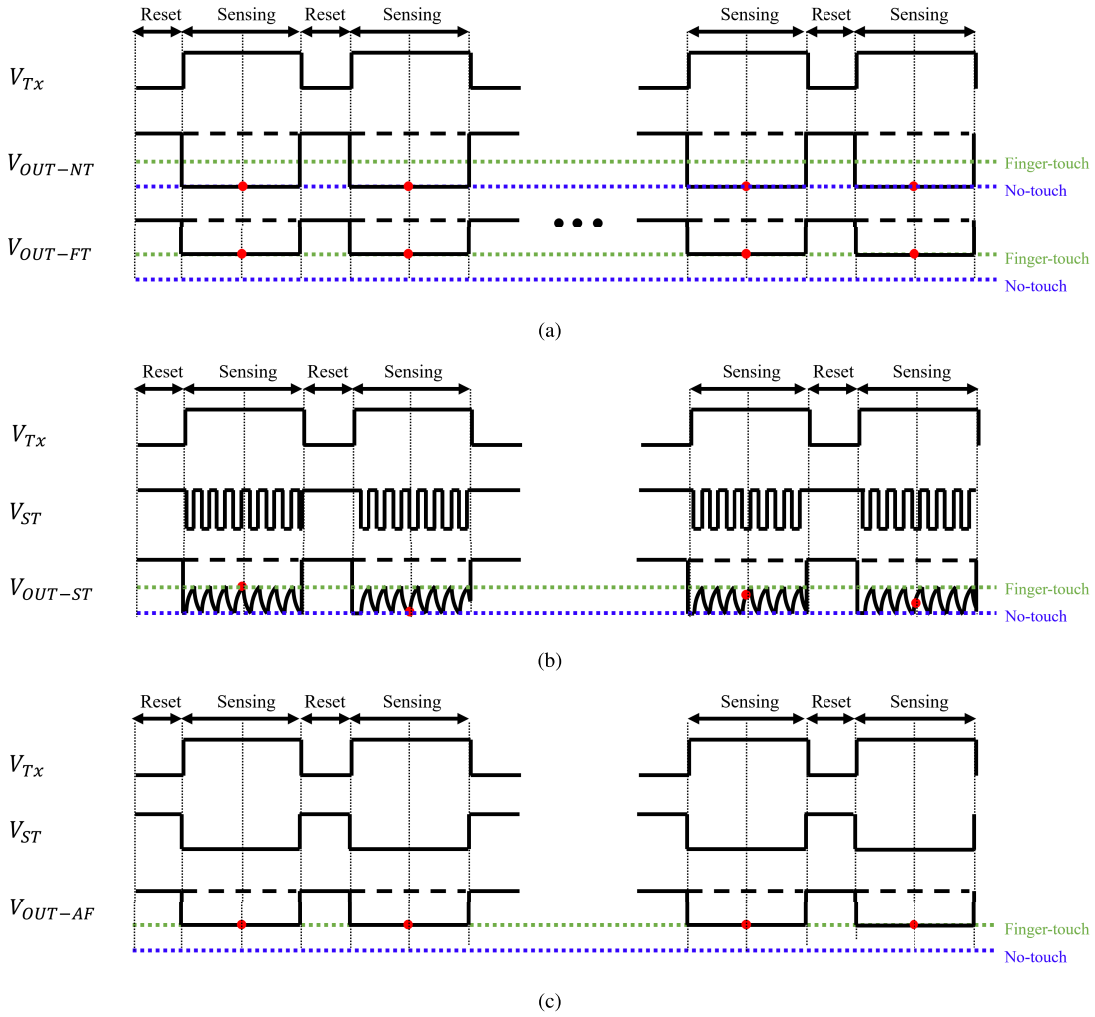

FIGURE 3. The output voltage waveforms of Rx circuit. (a) No-touch case and finger-touch case. (b) Stylus-touch case. (c) Artificial finger-touch case.

FIGURE 4. Proposed SVM-based touch data communication protocol.

FIGURE 5. Previous capacitive touch data communication protocol [16].

In the TSP side, finger-touch, stylus-touch, and data transmission can be discriminated as described in Fig. 6(a). No-touch and only finger-touch can be detected like any previous touch technologies. However, when a stylus-touch is detected, the TSP waits for a next touch event to decide whether this is only a stylus-touch or an initial code of the data transmission. If a finger-touch is detected with an artificial finger-touch at the same position, the next touch events are dealt with as the transmitted data. Else, it is handled as just a stylus-touch event. When the initial code is detected, then the received data are decoded as 1 for a stylus-touch and 0 for a no-touch until the terminal code.

Consequently, the proposed stylus can be used in two purposes as presented in Fig. 6(b). One is the touching tool for a TSP and the other is the data transmitter. When a *Touch* mode is selected, the TSP handles it as an touch input tool. The high frequency pulses are generated at the stylus output every Tx pulse of the TSP regardless of the data values. Whereas, in the *Data Transmission* mode, the stylus sends high frequency pulses as the value of 1 and then the artificial touch pulses as the value of 2 during the *Initial Code* period. In the next *Data Contents* period, the actual data stream is transmitted with one value among 0 and 1. After all data transmission is finished, the *Terminal Code* period of 0 and 2 is added to represent the end of the data transmission. The output voltage waveforms of the stylus are presented in Figs. 7(a), 7(b), 7(c), and 7(d) for *Touch*, *Initial Code*, *Data Contents*, and *Terminal Code*, respectively. As the Tx pulse (V_{Tx}) of a TSP is sensed

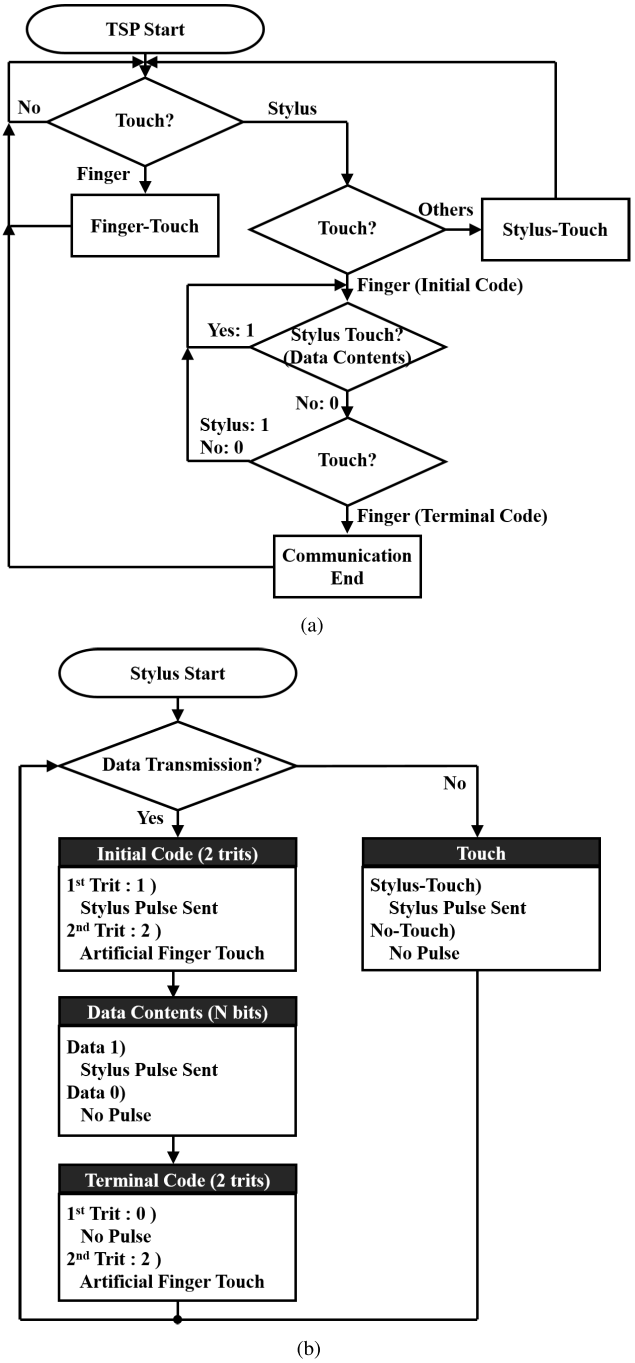

FIGURE 6. Operations of stylus and TSP. (a) Flowchart of stylus: When the *Data Transmission* mode is selected, initial code, data contents, and terminal code are transmitted in order. (b) Flowchart of TSP: TSP can discriminate finger-touch, stylus-touch, and data transmission.

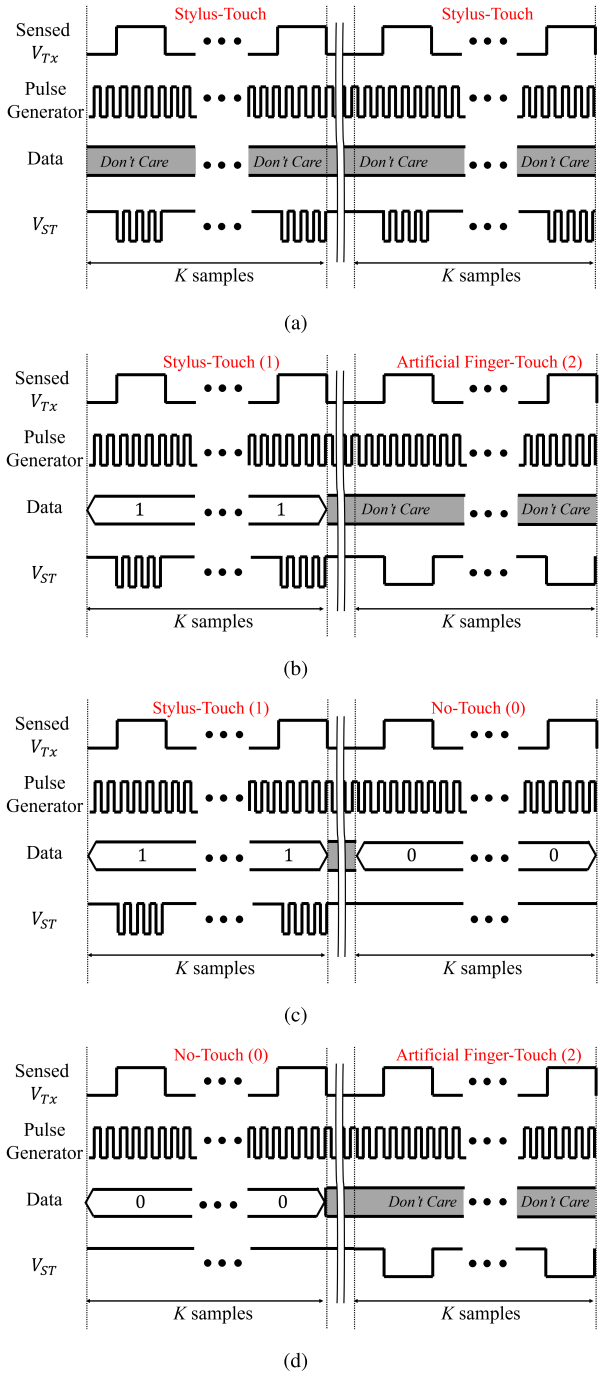

FIGURE 7. The output voltage waveforms of the stylus (a) *Touch* mode. (b) *Initial Code* period of *Data Transmission* mode. (c) *Data Contents* period of *Data Transmission* mode. (d) *Terminal Code* period of *Data Transmission* mode.

and used as the output enable signal in a stylus, the output pulses of V_{ST} become active only during the high intervals of the sensed V_{Tx}. The internal pulse generator gives rise to the high frequency pulses and one data detection requires K samples for the SVM classification.

Because the output pulses of the stylus should be synchronized to V_{Tx}, it is very important to sense V_{Tx} without missing pulses. The weak signals are transferred to the charge amplifier by the capacitor (C_S) formed between the Tx line of the TSP and the sensing electrode of the stylus and the logic-level pulses (V_{OUT}) are obtained via the comparator as shown in Fig. 8(a). The charge amplifier's output (V_O) is compared with a threshold voltage (V_{th}) leading to V_{OUT} equivalent to V_{Tx}. However, HUM noises may cause the common-mode drift of V_O. During one reporting period that is equal to one symbol period, these drifts make some V_{Tx}

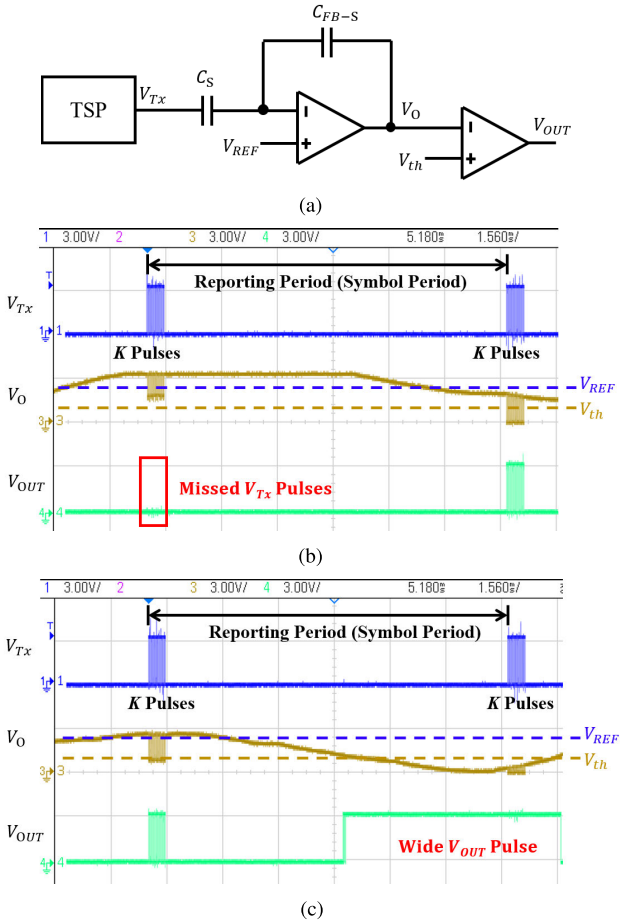

FIGURE 8. Sensing of V_{Tx} to synchronize the output of the stylus. (a) Sensing circuit base on charge amplifier and comparator. (b) Missed V_{Tx} pulses by upward common-mode drift. (c) Abnormally wide V_{OUT} pulses by downward common-mode drift.

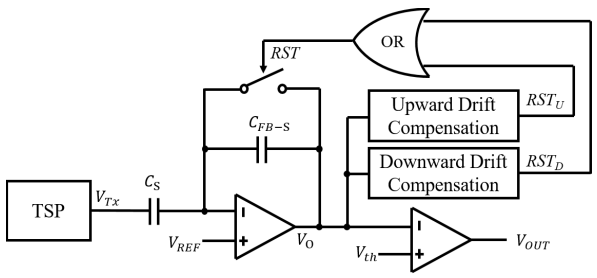

FIGURE 9. Full sensing circuit architecture to compensate for upward and downward common-mode drifts.

pulses missed or abnormally wide V_{OUT} pulses generated as presented in Figs. 8(b) and 8(c), respectively, which leads to the communication errors.

To address this drift issue, a reset switch is added to return the common-mode voltage to the target level (V_{REF}) by means of two compensation circuits for upward and downward common-mode drifts when V_O departs from the proper voltage region as illustrated in Fig. 9. Two compensation blocks generate reset signals (RST_U, RST_D) for upward and downward drifts and the final reset signal (RST) is provided by the OR operation of RST_U and RST_D.

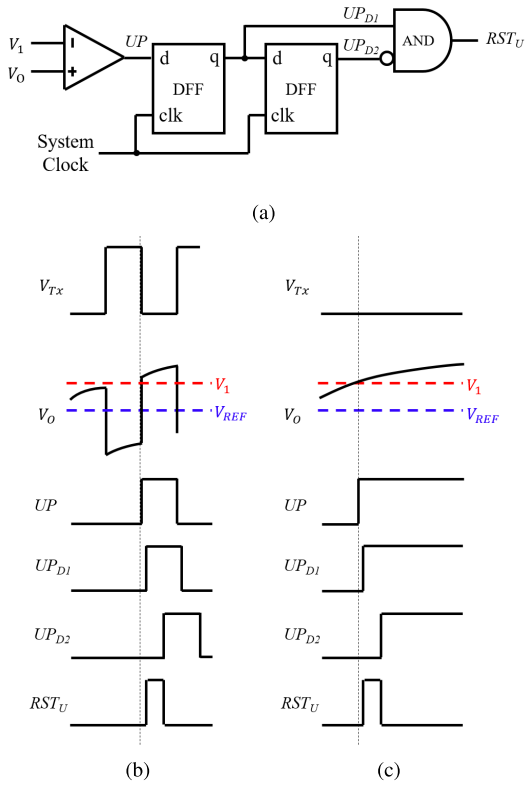

FIGURE 10. Upward drift compensation. (a) Compensation circuit diagram. (b) Compensation during V_{Tx} pulses. (c) Compensation during periods without V_{Tx} pulses.

In the upward drift compensation circuit expressed in Fig. 10(a), V_O is compared with V_1 that is set to higher than V_{REF}. Because V_O has the inverted waveform of V_{Tx}, the upward drift is detected during low voltage periods of V_{Tx} pulses. In the period of V_{Tx} pulses shown in Fig. 10(b), when V_O becomes higher than V_1, the comparator output pulse (UP) is sampled by two cascaded D flip-flops (DFFs) with UP_{D1} and UP_{D2} at the higher frequency system clock than Tx pulses. Finally, the reset pulse (RST_U) with the pulse width equal to the period of the system clock appears by the AND gate of UP_{D1} and inverted UP_{D2}, turning the reset switch on to remove the common-mode drift. For the interval between groups of K V_{Tx} pulses where no pulses exist, the upward drift is compensated for in the same way as illustrated in Fig. 10(c).

For the downward drift, a counter is added to compensate for the interval without V_{Tx} pulses as presented in Fig. 11(a). When V_{Tx} pulses exist, V_O is compared with V_2 that is determined between V_{th} and V_{REF} as illustrated in Fig. 11(b). Then, a reset pulse (RST_{D1}) is generated every the low level interval between V_{Tx} pulses. Whereas, because no V_{Tx} pulses exist between groups of K V_{Tx} pulses, another reset pulse (RST_{D2}) is given rise to every $N + 1$ system clocks counted by the additional counter as depicted in Fig. 11(c). Because RST_{D1} resets the counter to 0 every period of V_{Tx} pulses ($M + 1$) that is smaller than $N + 1$, RST_{D2} pulses appear only during the interval without V_{Tx} pulses. A final reset

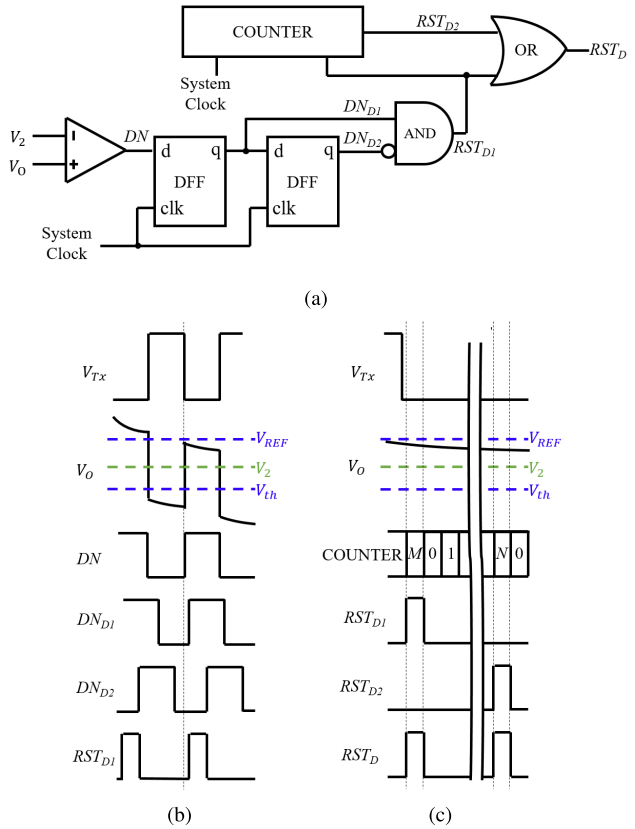

FIGURE 11. Downward drift compensation. (a) Compensation circuit diagram. (b) Compensation during V_{Tx} pulses. (c) Compensation during periods without V_{Tx} pulses: In these periods, RST_D is repeatedly given rise to every $N+1$ clocks by the internal counter. N is given to be larger than M that is the estimated period of the V_{Tx} pulse.

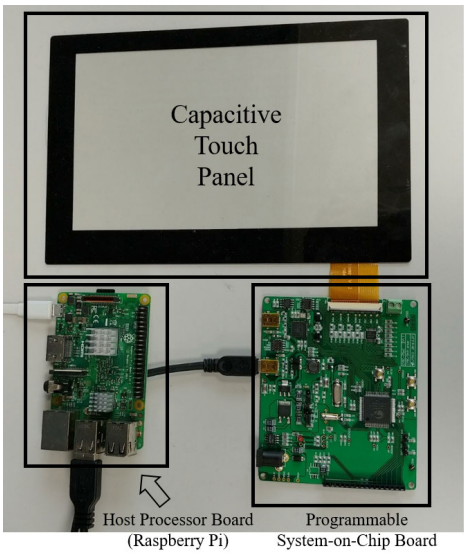

FIGURE 12. Evaluation setup of a proposed contact-based data receiver.

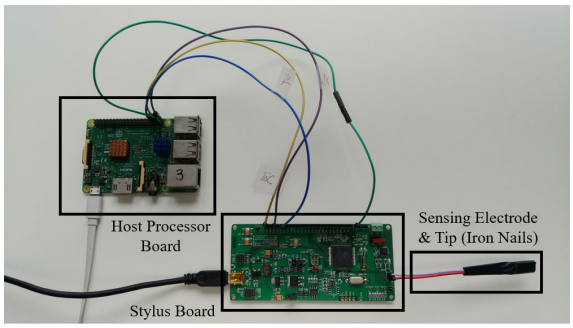

FIGURE 13. Evaluation setup of a proposed data transmitter.

signal (RST_D) is constructed via the OR gate, setting V_O of the charge amplifier to V_{REF}.

III. EXPERIMENT

The overall evaluation is conducted at the similar setup to the previous SVM-based touch system [14]. A proposed contact-based data receiver consists of 8-inch capacitive TSP, programmable system-on-chip board, and host processor board as shown in Fig. 12. One Tx line and one Rx line of the TSP are respectively driven and sensed to verify the proposed data communication technology. A programmable system-on-chip board provides the contact point of a Rx line, includes a level shifter integrated circuit (IC) to drive the Tx line at 5 V [18], and a programmable system-on-chip (Cypress Semiconductor PSoC 5LP) [19] to give rise to Tx pulses of 3.3 V and senses the voltage sequence on a Rx line by means of charge amplifier with C_{FB} of 3 pF and 8-bit ADC. The mutual capacitance of a cross area between a Tx line and a Rx line is estimated as 1.8 pF. Through a universal serial bus (USB), the digitally converted data are transferred to a host processor board that runs the SVM algorithm to differentiate three touch modes. A Raspberry Pi board (Raspberry Pi Foundation Raspberry Pi 3) [20] is used as a host processor board.

A proposed data transmitter, that is, a stylus is also built with stylus board and host processor board as shown in Fig. 13. A tip and a sensing electrode are made of iron nails with a diameter of 5 mm. The stylus senses Tx pulses through a capacitive coupling between stylus' sensing electrode and TSP's Tx line. The stylus board amplifies the sensed Tx pulses that are used to control the tip output timing with the output of a pulse generator. The voltage level at a tip is controlled by a level shifter IC in the stylus board and its frequency is set at 315 kHz. The stylus capacitance of a cross area between a tip and a Rx line is estimated as 0.4 pF.

$$\textit{Reporting rate} = \frac{f_{Tx}}{K \times N_{Tx}} = \frac{32000}{16 \times 20} = 100(\text{Hz}). \quad (1)$$

The frequency of Tx pulses (f_{Tx}) is 32 kHz that leads to 100 Hz reporting rate as described in Eq. (1). N_{Tx} and N_{Rx} that are the numbers of Tx and Rx lines are assumed to be 20 and 16, respectively [18]. The number of samples for SVM is 16 and support vectors are extracted from 3×10^6 training data sequences that are 10^6 sequences for each touch case. The smaller number of samples for SVM leads to higher reporting rate and data rate [14]. However, because the larger number of samples improves the bit error rate (BER) and the existing TSP technologies are using around 20 samples [18],

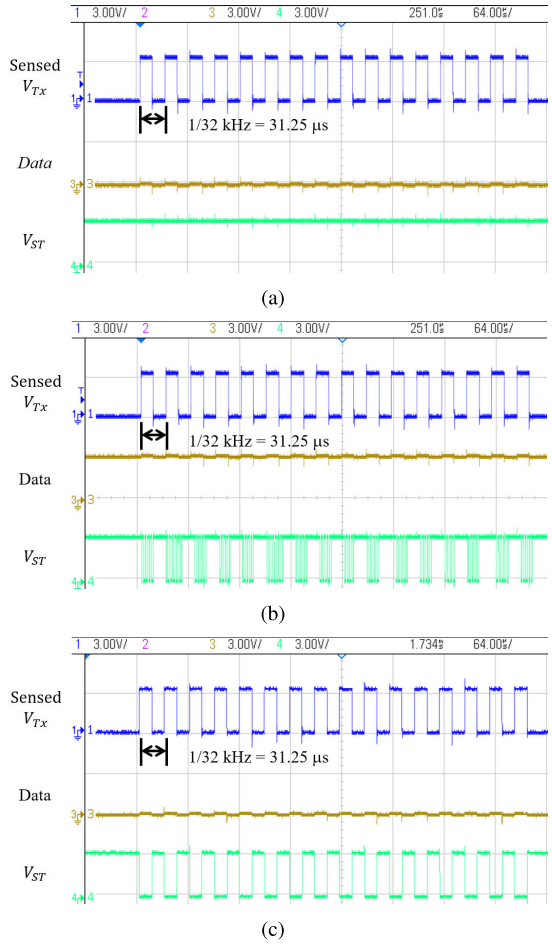

FIGURE 14. Measured waveforms of sensed V_{Tx}, *Data*, and V_{ST}. (a) No-touch. (b) Stylus-touch. (c) Artificial finger-touch.

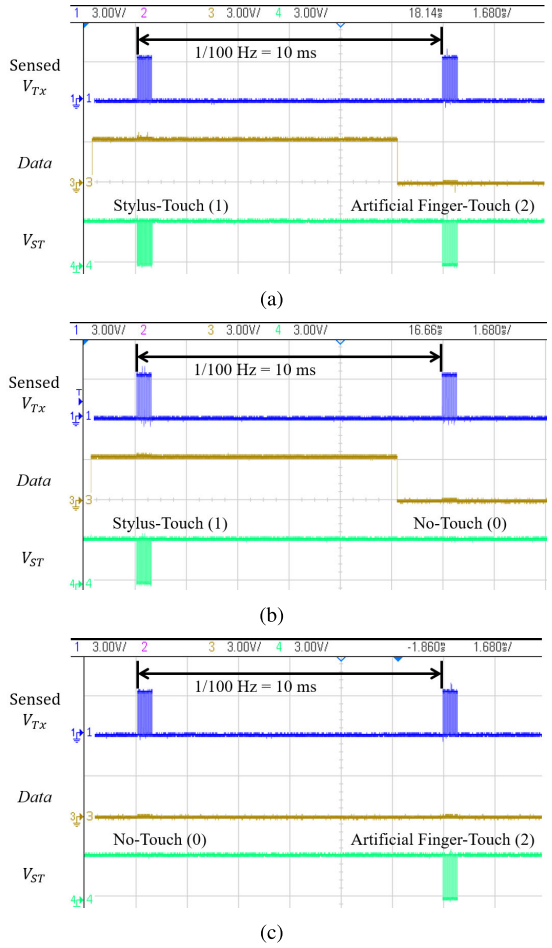

FIGURE 15. The measured waveforms for the proposed data transmission protocol. (a) Initial code period. (b) Data contents period. (c) Terminal code period.

16 samples are selected to verify the feasibility of the proposed scheme. 32 kHz of Tx pulses is determined by considering the maximum data rate that can be supported by the USB modules in programmable system-on-chip board and host processor board. When the data transmission is carried out in the progressive scanning way like the touch position processing, the resultant data rate is 100 bps. Because the number of extracted support vectors are 25 and their dimensions are equal to K, the proposed SVM classifier can be implemented by the simple matrix multiplication of support vector matrix of $25 \times K$ and input matrix of $K \times N_{Rx}$ for intersection points of one Tx line.

The reporting rate of the proposed one is independent of N_{Rx} because all Rx lines are sampled by one ADC of the high sampling rate (f_{ADC}) for a Tx pulse. The sampling rate is obtained as Eq. (2) where the factor of 2 is added with consideration of the 50 % duty ratio of the Tx pulse. If the higher duty ratio is in use, the resultant smaller factor than 2 can lead to the reduction on the sampling rate. In this evaluation setup, since this evaluation is conducted for one Rx line, the ADC samples the output voltage of the charge amplifier at 32 kHz that is the same frequency as f_{Tx}.

$$f_{ADC} = f_{Tx} \times N_{Rx} \times 2 = 1.024(\text{MHz}). \quad (2)$$

The measured waveforms of V_{ST} for no-touch, stylus-touch, and artificial finger-touch are presented in Figs. 14(a), 14(b), and 14(c), respectively. The no-touch maintains V_{ST} at the constant voltage, the stylus-touch generates high frequency pulses during the high voltage interval of sensed V_{Tx} pulses, and the artificial finger-touch provides inverted ones of sensed V_{Tx} pulses. The binary data waveform (*Data*) is also measured to show that 1 and 0 are stylus-touch and no-touch while the binary data is meaningless for the artificial finger-touch.

The data transmission protocol is also measured as shown in Figs. 15(a), 15(b), and 15(c) for initial code, data contents, and terminal code. In addition, the drift compensation blocks of the Tx pulse sensing circuit are also verified as shown in Fig. 16, where V_{th}, V_2, V_{REF}, and V_1 are 1.6 V, 2.0 V, 2.4 V, and 2.8 V, respectively. To generate *RST* pulses without missing one, two or more positive edges of the system clock should exist within a low voltage period of Tx pulses, that is, more than 4 positive edges in a period of Tx pulses (31.25 μs). Thus, the system clock of the compensation circuit is set to be 200 kHz that is about 6 times as high as Tx pulses leading to *RST* pulses of 5 μs. In the first red-box (Comp1), the upward drift at V_O causes a *RST* pulse and then the common-mode

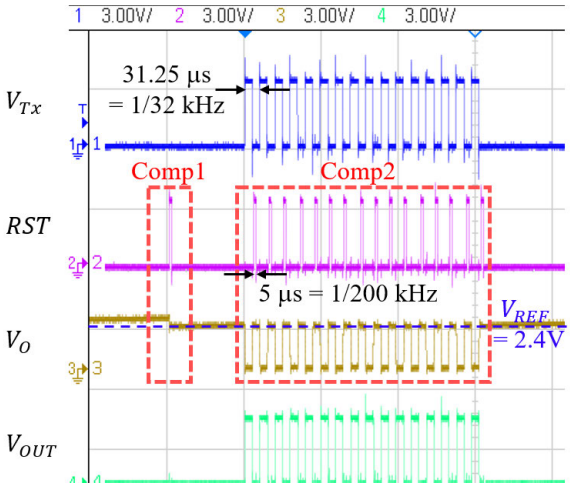

FIGURE 16. The measured waveform of the drift compensation in the Tx pulse sensing circuit. In the first red-box, the upward drift at V_O causes the pulse of *RST* and then the common-mode of V_O returns to V_{REF}. In the second red-box, the downward drift compensation block generates *RST* pulses every the low voltage interval between Tx pulses.

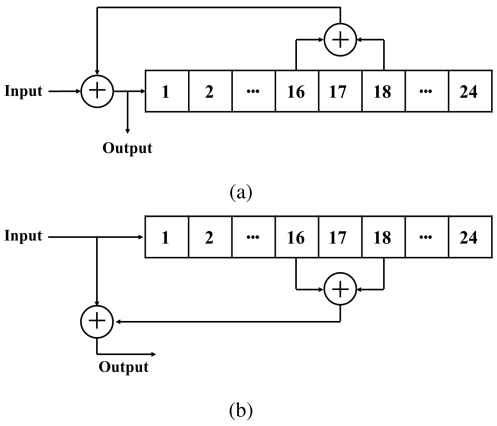

FIGURE 17. Self-synchronous scrambler and descrambler with the polynomial of $1+x^{-16}+x^{-18}$ for random binary data generation and recovery. (a) Self-synchronous scrambler (b) Self-synchronous descrambler.

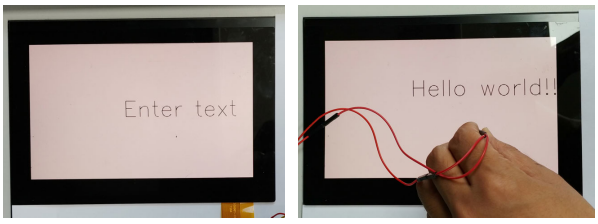

FIGURE 18. Example of the text transmission application with the proposed contact-based communication scheme. (a) The command of "Enter text" is shown in a display that is ready to receive the text data. (b) The stylus sends the data of "Hello world!!" and then the display presents the received text on a screen.

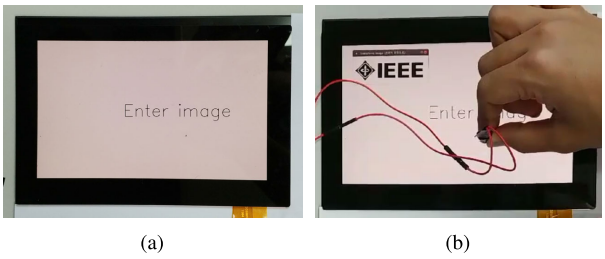

FIGURE 19. Image transmission by the proposed contact-based data communication. (a) The command of "Enter image" is presented in a display. (b) A stylus sends the image data on a screen and then the image of a IEEE logo appears on the top-left position.

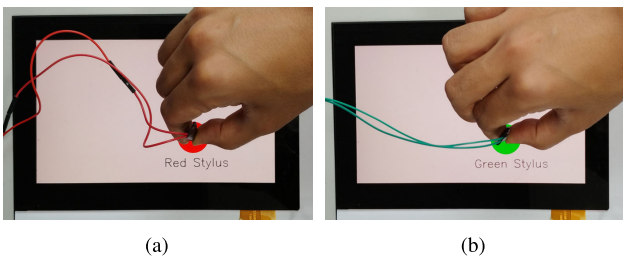

FIGURE 20. Stylus identification example with the proposed scheme. (a) The red-line stylus' contact is detected and then a red circle is displayed. (b) The green-line stylus' touch is sensed and then a green circle is shown.

of V_O returns to V_{REF} of 2.4 V. The second red-box (Comp2) shows that the downward drift compensation block generates *RST* pulses every low voltage interval between Tx pulses.

To measure the performance of the proposed communication method, self-synchronous scrambler and descrambler with polynomial of $1+x^{-16}+x^{-18}$ are used for random data generation and recovery as depicted in Figs. 17(a) and 17(b). The binary stream of 1's is randomized by the scrambler and sent through a tip of the stylus. Then, the receiver of the TSP side recovers the original binary sequence of 1's by the descrambler. Since all recovered binary data must be 1 that is the input of the scrambler, the BER is estimated by counting the number of zeros in the output of the descrambler. When the data communication is conducted without the proposed common-mode drift compensation block, it is observed that every received data are improperly recovered, that is, the BER is equal to 1. However, in the experiment with the compensation circuit, 10^7 data are successfully transmitted and received through scrambler and descrambler without any errors. In other words, it is ensured that the resultant BER is less than 10^{-7}. The BER performance for K of 8 is also measured at the data rate of 200 bps. As mentioned above, the higher BER of 5×10^{-6} is achieved, that is, 50 errors among 10^7 samples.

IV. APPLICATIONS

The proposed data communication system can be applied to various data transmission as well as stylus identification. When the display presents the command of 'Enter text' on a screen like Fig. 18(a), the data of "Hello world!!" are sent from the stylus and then, as shown in Fig. 18(b), that data appear on the display after the whole data transmission is completed.

Similarly, it can be also applied to image transmission. First, the command of 'Enter image' is displayed in Fig. 19(a). Then, the stylus sends the image data of a

IEEE logo that appears on the top-left region of the screen in Fig. 19(b).

In addition to text and image data transmission, it is possible to identify multiple stylus pens with the proposed technology. For example, two stylus modules transmit different identification codes from each other that allow the display to find out which stylus is placed on a screen. In Fig. 20(a), a red circle is displayed when the red-line stylus is used. Whereas, the green circle is shown in Fig. 20(b) when the green-line stylus is touched.

V. CONCLUSION

This paper proposes a contact-based data communication scheme that utilizes the SVM-based finger and stylus discrimination TSP technology. In addition to no-touch and stylus-touch, an artificial finger-touch is supported to indicate beginning and end of the data content transmission. Two levels of the binary data are represented by no-touch and stylus-touch while artificial finger-touches are included only in initial and terminal codes to differentiate them from the data contents with very short lengths. Because Tx pulses of the TSP must be sensed without missing ones, the drift compensation blocks are implemented in the sensing circuit. The overall transmitter and receiver systems are verified with capacitive TSP, programmable system-on-chip board, and host processor board. It is ensured that the proposed data communication system can support the data rate of higher than 100 bps with low BER of 10^{-7} or less, compared to the data rates of several bps at previous approaches.

REFERENCES

[1] T.-H. Hwang, W.-H. Cui, I.-S. Yang, and O.-K. Kwon, "A highly area-efficient controller for capacitive touch screen panel systems," *IEEE Trans. Consum. Electron.*, vol. 56, no. 2, pp. 1115–1122, May 2010.
[2] C. Luo, M. A. Borkar, A. J. Redfern, and J. H. McClellan, "Compressive sensing for sparse touch detection on capacitive touch screens," *IEEE Trans. Emerg. Sel. Topics Circuits Syst.*, vol. 2, no. 3, pp. 639–648, Sep. 2012.
[3] I. S. Yang and O. K. Kwon, "A touch controller using differential sensing method for on-cell capacitive touch screen panel systems," *IEEE Trans. Consum. Electron.*, vol. 57, no. 3, pp. 1027–1032, Aug. 2011.
[4] J.-H. Yang, S.-H. Park, J.-M. Choi, H.-S. Kim, C.-B. Park, S.-T. Ryu, and G.-H. Cho, "A highly noise-immune touch controller using filtered-delta-integration and a charge-interpolation technique for 10.1-inch capacitive touch-screen panels," in *IEEE ISSCC Dig. Tech. Papers*, Feb. 2013, pp. 390–391.
[5] S. Heo, H. Ma, J. Song, K. Park, E.-H. Choi, J. J. Kim, and F. Bien, "72 dB SNR, 240 Hz frame rate readout IC with differential continuous-mode parallel architecture for larger touch-screen panel applications," *IEEE Trans. Circuits Syst. I, Reg. Papers*, vol. 63, no. 7, pp. 960–971, Jul. 2016.
[6] S.-H. Park, H.-S. Kim, J.-S. Bang, G.-H. Cho, and G.-H. Cho, "A 0.26-nJ/node, 400-kHz Tx driving, filtered fully differential readout IC with parasitic RC time delay reduction technique for 65-in 169 × 97 capacitive-type touch screen panel," *IEEE J. Solid-State Circuits*, vol. 52, no. 2, pp. 528–542, Feb. 2017.
[7] N. Miura, S. Dosho, H. Tezuka, T. Miki, D. Fujimoto, T. Kiriyama, and M. Nagata, "A 1 mm pitch 80×80 channel 322 Hz frame-rate multitouch distribution sensor with two-step dual-mode capacitance scan," *IEEE J. Solid-State Circuits*, vol. 50, no. 11, pp. 2741–2749, Nov. 2015.
[8] M. Badaye and R. R. Schediwy, "Passive stylus for capacitive sensors," U.S. Patent 8 125 469, Feb. 28, 2012.
[9] S. Vuppu, D. Cranfill, M. Olley, and M. Valentine, "Active stylus for use with touch-sensitive interfaces and corresponding method,"U.S. Patent 8,766,954, Jul. 1, 2014.
[10] S. Shahparnia, K. Sundara-Rajan, Y. Ali, and I. Bentov, "Active stylus with high voltage," *U.S. Patent 8,866,767, Oct.*, vol. 21, 2014.
[11] R. Zachut, "Digitizer, stylus and method of synchronization therewith,"U.S. Patent 8,481,872, Jul. 9, 2013.
[12] J.-S. An, S.-H. Han, J. E. Kim, D.-H. Yoon, Y.-H. Kim, H.-H. Hong, J.-H. Ye, S.-J. Jung, S.-H. Lee, and J.-Y. Jeong, "9.6 a 3.9 khz-frame-rate capacitive touch system with pressure/tilt angle expressions of active stylus using multiple-frequency driving method for 65' 104× 64 touch screen panel," in *IEEE ISSCC Dig. Tech. Papers*, Feb. 2017, pp. 168–169.
[13] C. Chang-Hsien and C.-H. Huang, "Method for sensing fast motion, controller and electromagnetic sensing apparatus," U.S. Patent Appl. 14 472 345, Nov. 19, 2015.
[14] K.-H. Seol, S. Park, S.-J. Song, and H. Nam, "Finger and stylus discrimination scheme based on capacitive touch screen panel and support vector machine classifier," *Jpn. J. Appl. Phys.*, vol. 58, no. 7, 2019, Art. no. 074501.
[15] T. Vu, A. Baid, S. Gao, M. Gruteser, R. Howard, J. Lindqvist, P. Spasojevic, and J. Walling, "Capacitive touch communication: A technique to input data through devices' touch screen," *IEEE Trans. Mobile Comput.*, vol. 13, no. 1, pp. 4–19, Jan. 2014.
[16] M. Ogata, Y. Sugiura, H. Osawa, and M. Imai, "FlashTouch: Data communication through touchscreens," in *Proc. ACM SIGCHI*, 2013, pp. 2321–2324.
[17] S.-J. Song and H. Nam, "Sound-of-Tapping user interface technology with medium identification," *Displays*, vol. 53, pp. 54–64, 2018.
[18] J.-H. Yang, S.-H. Park, J.-Y. Jeon, H.-S. Kim, C.-B. Park, J.-C. Lee, J.-W. Kim, and G.-H. Cho, "A high-SNR area-efficient readout circuit using a delta-integration method for capacitive touch screen panels," in *SID Symp. Dig. Tech. Papers*, 2012, vol. 43, no. 1, pp. 1570–1573.
[19] *Cypress Semiconductor Corporation PSoC 5LP*. Accessed: Sep. 9, 2019. [Online]. Available: http://www.cypress.com/products/32-bit-arm-cortex-m3-psoc-5lp/
[20] *Raspberry Pi Foundation Raspberry Pi 3*. Accessed: Sep. 9, 2019. [Online]. Available: https://www.raspberrypi.org/documentation/

KI-HYUK SEOL received the B.S. degree from Kyung Hee University, Seoul, South Korea, in 2016, where he is currently pursuing the Ph.D. degree with the Department of Information Display. His current research interests are focused on low power integrated circuits and sensing methodologies of touch screen panel.

SEUNGJUN PARK received the B.S. degree from the Department of Information Display, Kyung Hee University, Seoul, South Korea, in 2018, where he is currently pursuing the M.S. degree. His current research is focused on integrated circuits for flat panel display applications.

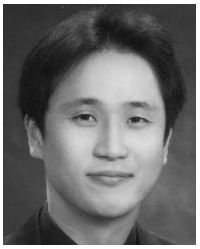

HYOUNGSIK NAM (M'10) received the B.S., M.S., and Ph.D. degrees in EECS from the Korea Advance Institute of Science and Technology (KAIST), Daejon, South Korea, in 1996, 1998, and 2004, respectively. In 2005, he joined Samsung Electronics as a Senior Engineer, where he had worked on Active-Matrix Liquid-Crystal Displays. He is currently an Associate Professor with the Department of Information Display, Kyung Hee University, Seoul, South Korea. His current research interests are low power technologies, integrated circuits, signal/user interfaces for flat panel displays, and machine learning application.